

# Realization of a Decoherence-free, Optimally Distinguishable Mesoscopic Quantum Superposition.

Francesco De Martini, Fabio Sciarrino, and Veronica Secondi

*Dipartimento di Fisica and Istituto Nazionale per la Fisica della Materia,  
Università "La Sapienza", Roma 00185, Italy*

## Abstract

We report the realization of an *entangled* quantum superposition of  $M \sim 12$  photons by a high gain, quantum-injected optical parametric amplification. The system is found so highly resilient against decoherence to exhibit directly accessible mesoscopic interference effects at normal temperature. By modern tomographic methods the non-separability and the quantum superposition are demonstrated for the overall mesoscopic output state of the dynamic "closed system". The device realizes the condition conceived by Erwin Schroedinger with his 1935 paradigmatic "Cat" apologue, a fundamental landmark in quantum mechanics.

Since the golden years of quantum mechanics the interference of classically distinguishable quantum states, first epitomized by the famous "*Schrodinger-Cat*" Apologue [1] has been the object of extensive theoretical studies and recognized as a major conceptual paradigm of physics [2]. In modern times the sciences of quantum information (QI) and quantum computation deal precisely with collective processes involving a multiplicity of interfering states, generally mutually entangled and rapidly de-phased by decoherence [3]. In many respects the implementation of this intriguing classical-quantum condition represents today an unsolved problem in spite of recent successful studies carried out mostly with atoms and ions [4,5]. The present work reports on a virtually decoherence-free scheme based on the quantum-injected optical parametric amplification (QI-OPA) of a single photon in a quantum superposition state of polarization ( $\pi$ ), i.e. a  $\pi$ -encoded qubit [6,7]. Conceptually, the method consists of transferring the well accessible condition of quantum superposition of a single photon qubit,  $N = 1$ , to a mesoscopic, i.e., multi-photon amplified state  $M \gg 1$ , here referred to as a "mesoscopic qubit" (M-qubit). This can be done by injecting in the QI-OPA the 1-photon qubit,  $\alpha |H\rangle + \beta |V\rangle$ , here expressed in terms of two orthogonal  $\pi$ -states, e.g. horizontal and vertical linear  $\pi$ :  $|H\rangle, |V\rangle$ . In virtue of the general *information preserving* property of the OPA, the generated state is found to be entangled and to keep the *same* superposition character and the interfering properties of the injected qubit [6]. Since the present scheme realizes the deterministic  $1 \rightarrow M$  *universal optimal quantum cloning machine* (UOQCM), i.e. able to copy *optimally* any unknown input qubit into  $M \gg 1$  copies with the same "fidelity", the output state will be necessarily affected by *squeezed-vacuum noise* arising from the input vacuum field.

Let's refer to the apparatus: Fig. 1. The active element was a nonlinear (NL) crystal slab (BBO:  $\beta$ -barium borate), 1.5 mm thick cut for Type II phase-matching, able to generate by spontaneous parametric down conversion (SPDC)  $\vec{\pi}$ -entangled photons pairs. The OPA *intrinsic phase* was set as to generate by SPDC *singlet* states on the output modes, a condition assuring the *universality* of the present cloning transformation [6,8–10]. The excitation source was a Ti:Sa Coherent MIRA mode-locked laser further amplified by a Ti-Sa

regenerative REGA device (**A**) operating with pulse duration  $180fs$  at a repetition rate  $250kHz$ , average power  $1W$ . By (**A**) the OPA nonlinear (NL) "gain"  $g$  was enhanced by a factor  $\simeq 17$  respect to earlier experiments [8–10]. The output beam, frequency doubled by second harmonic generation (SHG) provided the excitation beam with UV wavelength (wl)  $\lambda_P = 397.5nm$  and energy per pulse  $E_{UV}^{HG} = 1\mu J$ . The "seed" photons pairs were emitted, with a coherence time  $\approx 500fs$ , by a OPA process acting towards the right hand side (r.h.s.) of Fig.1 with equal wl's  $\lambda = 795nm$  over two spatial modes  $-\mathbf{k}_1$  and  $-\mathbf{k}_2$  owing to a SPDC process excited by the UV beam associated with mode  $-\mathbf{k}_p$  with wl  $\lambda_p$ . The UV beam was back-reflected over the mode  $\mathbf{k}_p$  onto the NL crystal by a spherical mirror  $\mathbf{M}_p$ , with  $\mu$ -metrically adjustable position  $\mathbf{Z}$ , thus exciting the main OPA "cloning" process towards the left hand side of Fig.1. By the combined effect of two adjustable optical UV wave-plates (wp's) ( $\lambda/2 + \lambda/4$ ) acting on the projections of the linear polarization  $\pi_p^{UV}$  on the optical axis of the BBO crystal for the  $-\mathbf{k}_p$  and  $\mathbf{k}_p$  excitation processes, the "seed" SPDC excitation was always kept at a low level while driving the main OPA to a large gain ( $HG$ ) regime. Precisely, by smartly unbalancing the orientation of the axes of the UV  $wp$ 's, the SPDC emission probability towards the r.h.s. of Fig.1 of 2 simultaneous photon pairs was always kept below the one of single pair emission by a factor  $\sim 3 \times 10^{-2}$ . One of the photons of the "seed" SPDC pair, back-reflected by a fixed mirror  $\mathbf{M}$ , was *re-injected* after a  $\vec{\pi}$ -flipping by a  $\lambda/4$  wp, onto the NL crystal over the input mode  $\mathbf{k}_1$ , while the other photon emitted over mode  $(-\mathbf{k}_2)$  excited the detector  $D_T$ , the *trigger* of the overall *conditional* experiment. The entangled state of the "seed" pair after  $M$ -reflection and  $\vec{\pi}$ -flipping was:  $|\Phi^-\rangle_{-k2,k1} = 2^{-1/2} (|H\rangle_{-k2} |H\rangle_{k1} - |V\rangle_{-k2} |V\rangle_{k1})$ . In virtue of the nonlocal correlation acting on the "seed" modes  $-\mathbf{k}_1$  and  $-\mathbf{k}_2$ , the input qubit was prepared on mode  $\mathbf{k}_1$  in the *pure* state  $|\Psi\rangle_{in} = \alpha |H\rangle_{k1} + \beta |V\rangle_{k1}$ ,  $|\alpha|^2 + |\beta|^2 = 1$  by the combined action of the  $\lambda/2$  wp, of  $\lambda/4$  wp ( $WP_T$ ), of the adjustable *Babinet Compensator* ( $B$ ) and of a polarizing beam-splitter ( $PBS_T$ ) acting on mode  $-\mathbf{k}_2$ . This device allowed all orthogonal transformations  $\hat{U}_X$ ,  $\hat{U}_Y$ ,  $\hat{U}_Z$  on the Bloch sphere of the input qubit: Fig.1, inset. The Quantum State Tomography (QST) devices  $T_T, T_i (i=1, 2)$  were equipped with equal single-photon fiber coupled SPCM-

AQR14-FC detectors ( $D$ ) and equal interference filters with bandwidth  $\Delta\lambda = 4.5nm$  were placed in front of each  $D$ : Fig.1-inset.

Let's re-write  $|\Psi\rangle_{in}$  in terms of Fock product states:  $|H\rangle_{k1} = |1\rangle_{1H} |0\rangle_{1V} |0\rangle_{2H} |0\rangle_{2V} \equiv |1, 0, 0, 0\rangle$ ;  $|V\rangle_{k1} = |0, 1, 0, 0\rangle$ , accounting for 1 photon on the input  $\mathbf{k}_1$  with different orthogonal  $\vec{\pi}'$ s and vacuum on the input  $\mathbf{k}_2$ . It evolves into the output state  $|\Psi\rangle = \hat{U} |\Psi\rangle_{in}$  according to the main OPA unitary  $\hat{U}$  process [10]. The output state  $\tilde{\rho} = (|\Psi\rangle \langle\Psi|)$  over the modes  $\mathbf{k}_1, \mathbf{k}_2$  of the QI-OPA apparatus is found to be expressed by the *M-qubit*:

$$|\Psi\rangle = \alpha |\Psi\rangle^H + \beta |\Psi\rangle^V \quad (1)$$

where:  $|\Psi\rangle^H = \sum_{i,j=0}^{\infty} \gamma_{ij} \sqrt{i+1} |i+1, j, j, i\rangle$ ,  $\gamma_{ij} \equiv \cosh^{-3} g (-\Gamma)^i \Gamma^j$ ,  $\Gamma \equiv \tanh g$ ,  $|\Psi\rangle^V = \sum_{i,j=0}^{\infty} \gamma_{ij} \sqrt{j+1} |i, j+1, j, i\rangle$ , being  $g$  the NL gain [8]. These interfering *entangled*, multi-particle states are *ortho-normal*, i.e.  $|\langle\Psi | \Psi\rangle^j|^2 = \delta_{ij}$   $\{i, j = H, V\}$  and *pure*, i.e. fully represented by the operators:  $\rho^H = (|\Psi\rangle \langle\Psi|)^H$ ,  $\rho^V = (|\Psi\rangle \langle\Psi|)^V$ . Hence the *pure* state  $|\Psi\rangle$  is a quantum superposition of two multi-photon *pure states* and bears the *same* superposition properties of the injected qubit. In addition, it is highly significant in the present context to consider the output *pure* state of the *overall* apparatus, including the "trigger" that enters in the dynamics through the Bell state  $|\Phi^-\rangle_{-k2, k1}$ . The state  $|\Sigma\rangle$ , commonly referred to as the "*Schroedinger Cat State*" [11], expresses the entanglement of all output modes  $\mathbf{k}_1, \mathbf{k}_2$  and  $-\mathbf{k}_2$ , thus eliciting a peculiar cause-effect dynamics within the overall "closed" system:

$$|\Sigma\rangle \equiv 2^{-1/2} (|H\rangle_{-k2} |\Psi\rangle^H - |V\rangle_{-k2} |\Psi\rangle^V) \quad (2)$$

In the pictorial context of the Cat apologue,  $|\Sigma\rangle$  expresses the correlations established within the "closed box" between the "microscopic" state of the decaying particle that triggers the release of the deadly poison and the "macroscopic" state of the threatened animal [1,2]. The *entanglement entropy*  $\mathcal{E}(|\Sigma\rangle)$  of  $\tilde{\rho}' \equiv |\Sigma\rangle \langle\Sigma|$  is expressed by the Von Neuman entropy of either the  $-k_2$  or *OPA* subsystem:  $\mathcal{E}(|\Sigma\rangle) = S(\tilde{\rho}_{-k2}) = S(\tilde{\rho}_{opa}) = 1$ , being  $\tilde{\rho}_{-k2} = Tr_{opa}(\tilde{\rho}')$ ,  $\tilde{\rho}_{opa} = Tr_{-k2}(\tilde{\rho}')$  and  $S(\tilde{\rho}_j) = -Tr(\tilde{\rho}_j \log_2 \tilde{\rho}_j)$  [12,10]. The maximal attainable value is  $\mathcal{E}(|\Sigma\rangle) = 1$  for the output bipartite system.

The experimental investigation of the multiphoton superposition and entanglement implied by Eqs 1, 2 was carried out by means of the  $T_i, T_T$  devices according to a "loss method" first applied to SPDC by [13]. The beams associated with the output modes  $\mathbf{k}_i (i=1, 2)$  were highly attenuated to the *single-photon* level by the two low transmittivity BS's ( $At$ ) in Fig.1. Since the bipartite entanglement affecting the multiphoton  $\mathbf{k}_i, (i=1, 2)$  also implies a correlation of the single photons detected on either modes and since it is impossible to create or enhance entanglement by *local* operations, e.g. by the loss mechanism acting over each mode, the entanglement detected at the *single-photon* level over  $\mathbf{k}_i, (i=1, 2)$  necessarily implies the same property to affect the same modes in the *multi-photon* condition. In agreement with the "loss method" we investigated by two different QST experiments the *reduced* density matrices  $\rho$  and  $\rho'$ , i.e. the *single-photon* counterparts of the pure, multi-photon states  $\tilde{\rho}, \tilde{\rho}'$  given by Eqs.1, 2. The experimental results, reported in Figs. 2, 3 respectively, are compared with the corresponding theoretical  $\rho^{th}$  and  $\rho'^{th}$  which have been calculated by a numerical algorithm performing the multiple tracing of  $\tilde{\rho}, \tilde{\rho}'$  over all photons discarded by the  $At$  devices on the modes  $\mathbf{k}_i (i = 1, 2)$ . Theoretical details on this most useful algorithm and on the overall experiment will be given in a forthcoming comprehensive paper [14]. In order to carry out the calculations properly, the maximum value of the "gain"  $g_{exp}$  and of the overall quantum efficiencies  $\eta_i$  of the detection apparatuses acting on  $\mathbf{k}_i (i = 1, 2)$  were measured. It was found:  $g_{exp} = 1.19 \pm 0.05$  and  $\eta_1 = (4.9 \pm 0.2)\%$ ;  $\eta_2 = (4.2 \pm 0.2)\%$ .

Let us now address the main goal of the present work, i.e. the detection and characterization of the output states. The interference (IF) character of the output field implied by the quantum superposition character of the input qubit  $|\Psi\rangle_{in} = 2^{-1/2}(|H\rangle + e^{i\varphi}|V\rangle)$  was detected simultaneously in the basis  $|\pm\rangle \equiv 2^{-1/2}(|H\rangle \pm |V\rangle)$  over the output "cloning" mode,  $\mathbf{k}_1$  and "anticloning",  $\mathbf{k}_2$  by the 2- $D$  coincidences  $[D_i, D_T]$  (square marks in Fig 1-inset) and  $[D_i^*, D_T]$  (circle marks) ( $i=1, 2$ ). Precisely, the IF fringe patterns shown in Fig.1 correspond to  $\hat{U}_Z$  transformations on the input Bloch sphere, i.e. implying changes of the phase  $\varphi$ . The fringe "visibility" ( $\mathcal{V}$ ) measured over  $\mathbf{k}_1$  was found to be gain-dependent  $\mathcal{V}_1^{th}(g) = (1 + 2\Gamma^2)^{-1}$  as predicted by theory [6]. The experimental value  $\mathcal{V}_1 = (32 \pm 1)\%$  should be compared with

the theoretical one:  $\mathcal{V}_1^{th}(g_{\text{exp}})=42\%$ . By setting  $g=\Gamma=0$  the effective visibility of the input qubit was measured:  $\mathcal{V}_{in} \approx 87\%$ . The  $\mathcal{V}$ -value for the  $\mathbf{k}_2$  mode  $\mathcal{V}_2=(13 \pm 1)\%$  should be compared with the theoretical:  $\mathcal{V}_2^{th} = 33\%$  [6]. These discrepancies are attributed to unavoidable walk-off effects in the NL slab spoiling the critical superposition of the injection and pump pulses in the bi-refractive active region. In the quantum-injected *HG* regime, the overall average number of the stimulated emission photons *per pulse* over  $\mathbf{k}_i(i=1,2)$  was found,  $M = (11.1 \pm 1.3)$ , a result consistent with the value of  $g$  measured by an entirely different experiment. Precisely, the average number of photons generated on the cloning mode was:  $M_C = 6.1 \pm 0.9$  and the average "fidelity", obtained by the corresponding  $\mathcal{V}$ -value on the same mode, was:  $F_C = (1 + \mathcal{V}_1)/2 = 66.2 \pm 0.5$ . Note that for  $M \rightarrow \infty$ , viz.  $g \rightarrow \infty$  and  $\Gamma \rightarrow 1$ , the "fringe visibility" and the "fidelity" attain the asymptotic values  $\mathcal{V}_1^{th} = \mathcal{V}_2^{th} = 33\%$  and  $F_C = F_{AC} = (2/3)$ . In the present experiment, in absence of reliable photon number-resolving detectors, the measurement of  $M$  and  $M_C$  was transformed into a detection rate measurement as  $\eta_1 \sim \eta_2 \ll 1$ .

A most insightful state analysis was provided by a full QST study of the output  $\rho$  and  $\rho'$ , as said. Figure 2 shows the QST analysis of the *reduced* output state  $\rho$  determined by the set of input  $|\Psi\rangle_{in}$ :  $\{|H\rangle, |V\rangle, |\pm\rangle\}$ . The experimental data  $\rho^{\text{exp}}$  shown by Fig. 2-**b**, were obtained by a 3-D coincidence method  $[D_T, D_1, D_2]$  for different settings of the QST setups  $T_i$ . The good agreement between theory and experiment is expressed by the measured average Uhlmann "fidelity":  $\mathcal{F}(\rho^{\text{exp}}, \rho^{th}) \equiv [Tr(\sqrt{\rho^{\text{exp}}} \rho^{th} \sqrt{\rho^{\text{exp}}})^{\frac{1}{2}}]^2 = (96.6 \pm 1.2)\%$ . In Fig. 2-**a, b** the structure of the  $4 \times 4$  matrices  $\rho$  shows the relevant quantum features of the output state. For instance, the highest peak on the diagonals expressing the quantum superposition of the input state shifts from the position  $|\phi\phi^\perp\rangle\langle\phi\phi^\perp|$  to  $|\phi^\perp\phi\rangle\langle\phi^\perp\phi|$  in correspondence with the OPA excitation by any set of orthogonal injection states  $\{|\phi\rangle, |\phi^\perp\rangle\}$ , i.e. represented by the maxima and minima of the IF fringe patterns of Fig.1, inset. The experimental patterns of Fig. 2-**b** obtained by injection of different basis sets  $\{|H\rangle, |V\rangle\}$  and  $\{|+\rangle, |-\rangle\}$  indeed confirm the "universality" of this process, i.e. reproducing identically for any couple of orthogonal input states. As expected, the IF fringe pattern of Fig 1-inset

was found to disappear in absence of the injection qubit (rhomb marks in Fig.1-inset) [14]. The application to all  $\rho$  matrices shown in Fig.2-**b** of the Peres-Horodecki Positive Partial Transpose (*PPT*) criterion ensures the non-separability of the reduced state  $\rho$  and then necessarily of the corresponding "true" *multiphoton* output state  $\tilde{\rho}$ , as said [15,13]. Indeed the minimal eigenvalue of the transpose of the "theoretical" matrices  $\rho^{th}$  of Fig. 2-**a** was found *negative*,  $\lambda_{\min} = -0.046$ , a result reproduced by all  $\rho^{\text{exp}}$  reported in Fig. 2-**b**. For instance for  $\rho^{\text{exp}}$  determined by  $|\Psi\rangle_{in} = |-\rangle$  it was found:  $\lambda = -0.014 \pm 0.0025$  for  $g_{\text{exp}} \sim 1.19$ . Let's turn our attention to the state  $\rho'$  correlating *all output* modes: Fig. 3-**b**. The QST reconstruction was achieved by the devices  $T_T, T_i$  again with a large fidelity:  $\mathcal{F}(\rho'^{\text{exp}}, \rho'^{th}) = (85.0 \pm 1.1)\%$ . The quantum superposition of the output state is expressed here by the off-diagonal elements of both matrices:  $\rho'^{th}, \rho'^{\text{exp}}$ . Once again, the nonseparability of  $\rho'$  for the bipartite system  $-\mathbf{k}_2$  and  $\{\mathbf{k}_1, \mathbf{k}_2\}$  was proved by the PPT method, a sufficient criterion for 3-qubit mixed states. Again, the minimal eigenvalue of the transpose of both matrices  $\rho'$  in Fig. 3 was found *negative*:  $\lambda'_{\min} = -0.024$  and  $\lambda'_{\text{exp}} = -0.021 \pm 0.004$ . This proves the nonseparability of the "true" tri-partite pure state  $\tilde{\rho}'$ , Eq.2, correlating the trigger and the multiphoton  $\mathbf{k}_i$  modes within the "closed box".

A striking property of the present system is its extreme resilience to de-coherence as shown by the interference patterns of Fig.1 [3]. Consequently, unlike other systems involving atoms or superconductors [4,5] the mesoscopic superposition is *directly accessible* at the output of the apparatus at *normal*, i.e. "room", temperature (T). This lucky result is partially attributed to the *minimum* Hilbert-Schmidt ( $d$ ) "distance" on the *phase-space* of the interfering states realized here:  $d(\rho^H; \rho^V) = \text{Tr}[(\rho^H - \rho^V)^2] = 2$  [16]. Since in our system the de-coherence can only be determined by stray reflection losses on the single output surface of the NL crystal, a number of photons in the range  $(10^2 \div 10^3)$  could be easily excited in quantum superposition. The limited, i.e. *optimal*, distinguishability of the mesoscopic states is attributed to our *single particle, cloningwise*  $\pi$ -measurement method. However, the *exact* distinguishability implied by the orthogonality of  $|\Psi\rangle^H$  and  $|\Psi\rangle^V$  could be possibly attained if any POVM identifying in a *cumulative fashion* all  $M$  particles involved in the

interference could be found.

In summary, we have demonstrated the quantum interference of *mesoscopic, orthonormal, pure* states in agreement with the original Schroedinger's proposal [1] and with our quantum theoretical results, Eqs.1, 2. In the near future, the adoption of "periodic-poled" nonlinearities is expected to further increase  $g$  by a factor  $\geq 2$  and then the value of  $M$  by at least an order of magnitude. On a conceptual side our system is expected to open a new trend of studies on the persistence of the validity of crucial laws of quantum mechanics for entangled mixed-state systems of increasing complexity [4], on the realization of GHZ processes and on the violation of Bell inequalities in the multi-particles regime [17]. In addition, our method may suggest a plausible signal-amplification model for the establishment of collective coherence effects in complex biological systems at normal T, e.g. within the search of any non-computable physical process in the self-conscious brain [18]. We thank Marco Caminati and Riccardo Perris for experimental help within the tomographic reconstructions and Serge Haroche, Peter Knight, Wojciech Zurek, Vlado Buzek and Wolfgang Schleich for enlightening discussions. Work supported by the FET EU Network on QI Communication (IST-2000-29681: ATESIT), INFN (PRA "CLON") and by MIUR (COFIN 2002).



## REFERENCES

- [1] E. Schroedinger, *Naturwissenschaften* **23**, 807-823 (1935).
- [2] A. Caldeira, *et al.*, *Physica A* **121**, 587 (1983); A. Leggett, *et al.*, *Phys. Rev. Lett.* **54**, 857 (1985).
- [3] W. Zurek, *Physics Today*, October 1991, pag.36.
- [4] M. Brune, *et al.*, *Phys. Rev. Lett.* **77**, 4887 (1996); A. Auffeves, *et al.*, *Phys. Rev. Lett.* **91**, 230405 (2003); P. Maioli, *et al.*, *Phys. Rev. Lett.* **94**, 113601 (2005).
- [5] C. Monroe, *et al.*, *Science* **272**, 1131 (1996); D. Leibfried, *et al.*, *Science* **304**, 1476 (2004), C.F. Roos, *et al.*, *Science* **304**, 1478 (2004).
- [6] F. De Martini, *Phys. Rev. Lett.* **81**, 2842 (1998). Larger values of  $\mathcal{V}_i^{th}$  are offered by less "universal" cloning schemes, e.g. by the mode-degenerate *phase-covariant* cloning: F. De Martini, *Phys. Lett. A* **250**, 15 (1998).
- [7] F. De Martini, *et al.*, *Phys. Rev. Lett.* **87**, 150401 (2001).
- [8] F. De Martini, *et al.*, *Nature (London)* **419**, 815 (2002).
- [9] F. De Martini *et al.* *Opt. Comm.* **179**, 581 (2000); A. Lamas-Linares, *et al.*, *Science* **296**, 712 (2002).
- [10] D. Pelliccia, *et al.*, *Phys. Rev. A* **68**, 042306 (2003); F. De Martini, *et al.*, *Phys. Rev. Lett.* **92**, 067901 (2004).
- [11] W.P.Schleich, *Quantum Optics in Phase Space* (Wiley, New York, 2001) Chs.11,16
- [12] C.H. Bennett, *et al.*, *Phys. Rev. A* **54**, 3824 (1996).
- [13] H.S. Eisenberg, *et al.*, *Phys. Rev. Lett.* **93**, 3901 (2004); G.A. Durkin, *et al.*, *Phys. Rev. A* **70**, 062305 (2004).
- [14] M. Caminati *et al.* (in preparation).

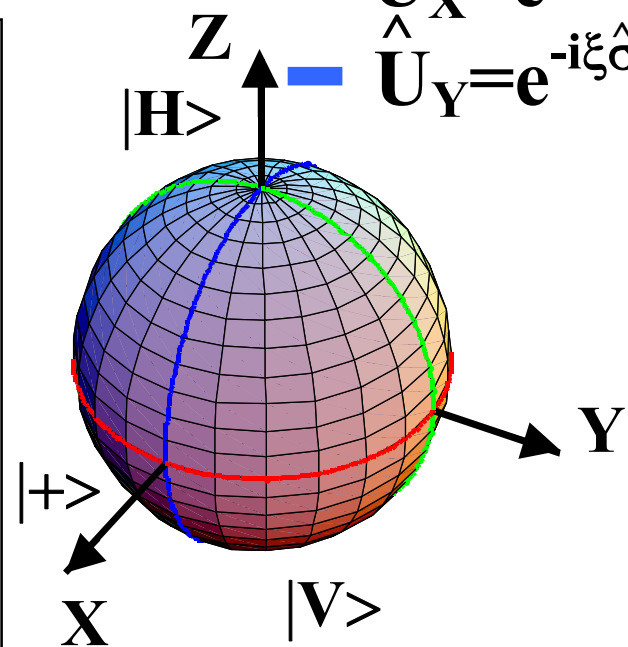
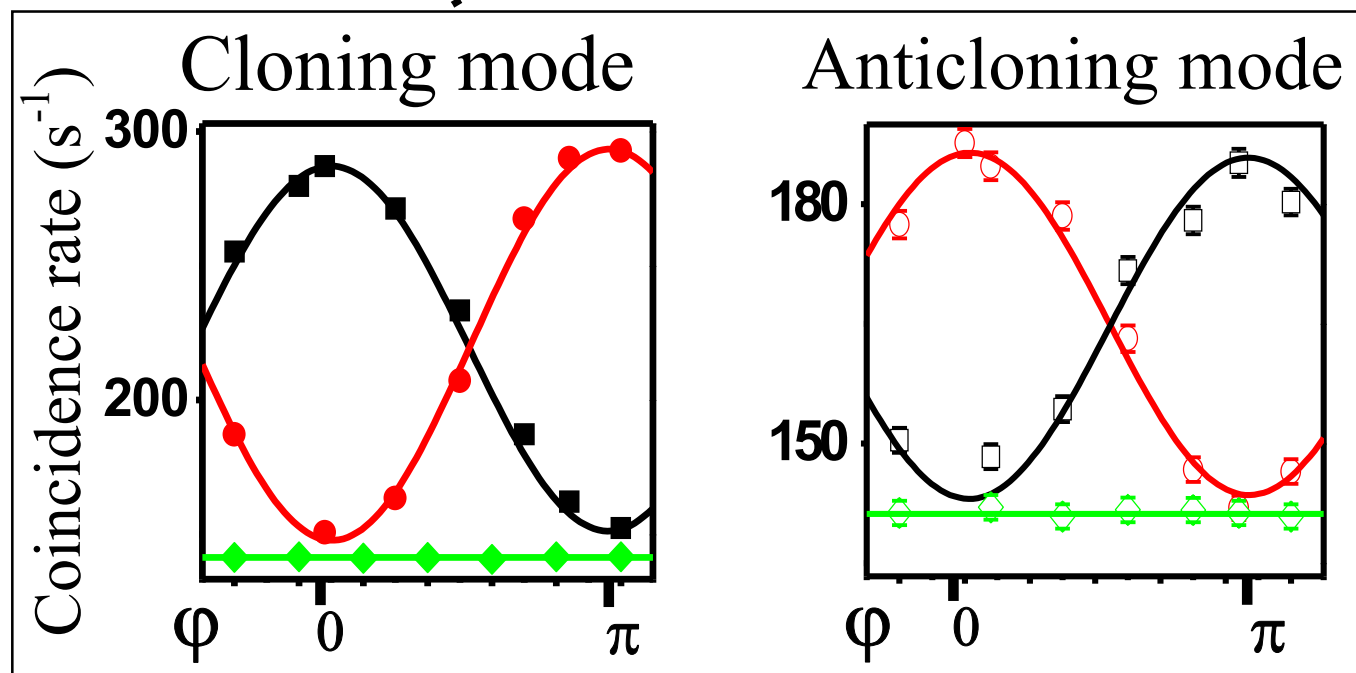
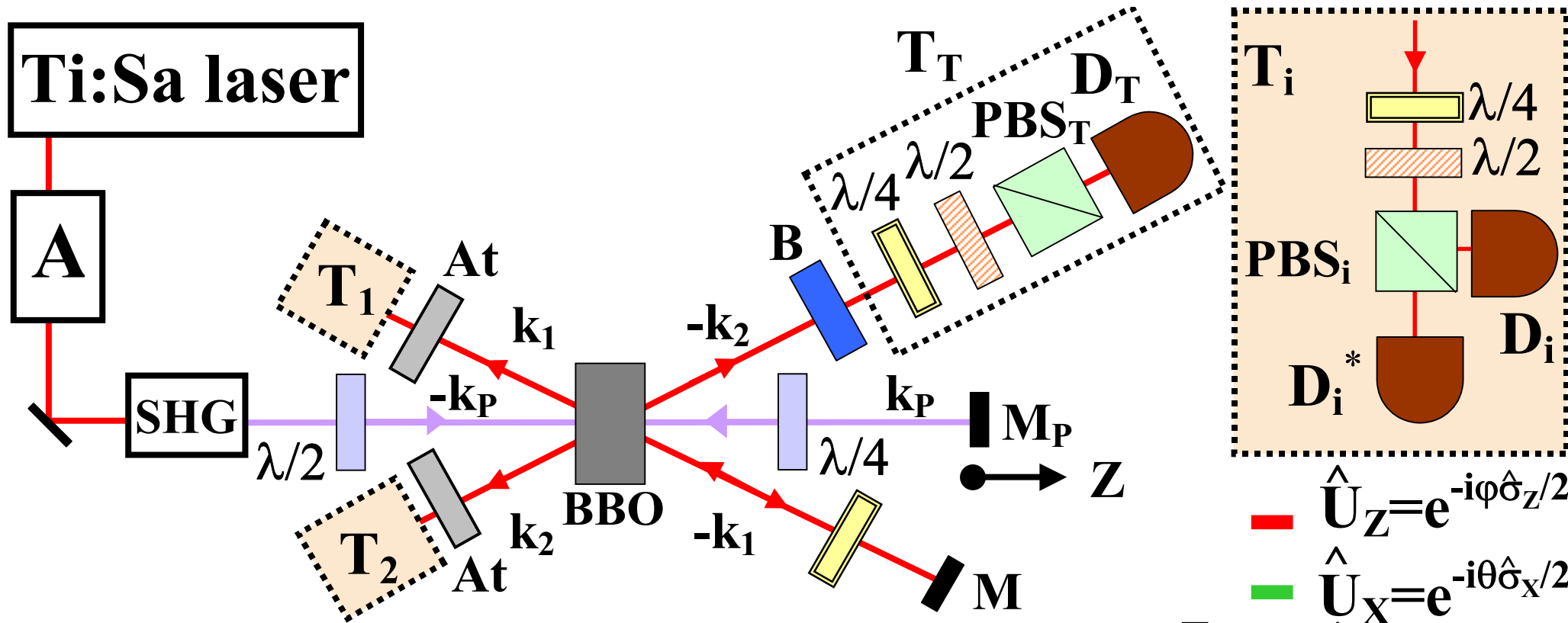
- [15] A. Peres, Phys. Rev. Lett. **77**, 1413 (1996).
- [16] M. Nielsen, *et al.*, *Quantum Computation and Information* (Cambridge, 2000) Ch9.
- [17] M.D. Reid, *et al.*, Phys. Rev. A **66**, 033801 (2002).
- [18] R. Penrose, *The Large, the Small and the Human Mind* (Cambridge University Press, 2000) Ch.3.

### Figure Captions

Figure 1. Layout of the *quantum-injected OPA* apparatus;  $T_i$ , ( $i = 1, 2$ ) Quantum State Tomographic (QST) setups; Bloch sphere representation of the input qubit. Inset: mesoscopic interference fringe patterns measured over the modes  $\mathbf{k}_i$  Vs the input phase  $\varphi$  for the  $\hat{U}_Z$  map. The continuous lines express the best fit results.

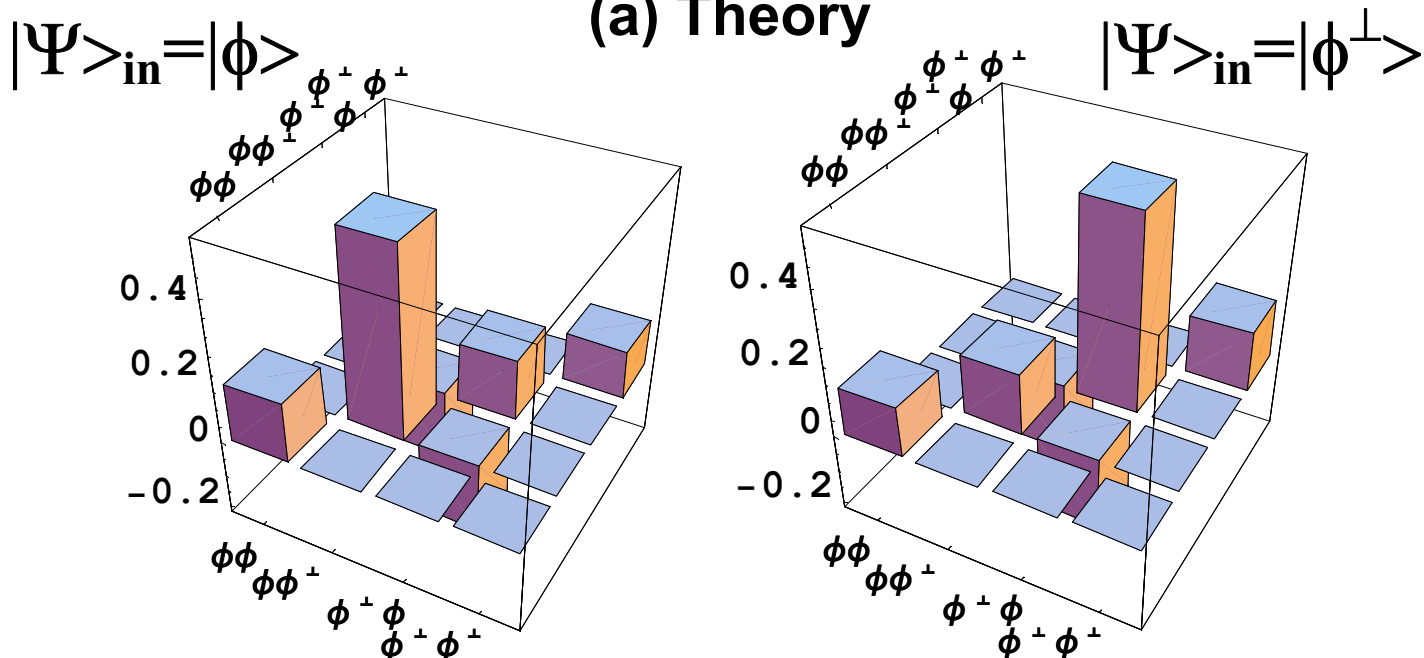
Figure 2. QST plots of the *reduced* output state over the 2 output modes  $\mathbf{k}_i$ , ( $i = 1, 2$ ) conditioned by the injection of a polarization qubit  $|\Psi\rangle_{in}$  on mode  $\mathbf{k}_1$ . (a) Theoretical simulation. (b) Experimental results. The imaginary components are negligible in the given scale.

Figure 3. QST plots of the reduced overall output state  $\rho^{th}$  over the 3 modes  $-\mathbf{k}_2$ ,  $\mathbf{k}_i$ , ( $i = 1, 2$ ) under the condition of lossy channels for the multiphoton modes  $\mathbf{k}_i$ . The experimental  $\rho'^{exp}$  was reconstructed by measuring 64 three-qubit observables and by applying a linear inversion reconstruction. Each QST run lasted 60s and yielded a maximum 1866 threefold counts for the  $|HHV\rangle$  projection. The uncertainties of the data were evaluated by a numerical simulation assuming Poissonian fluctuations. The imaginary plots are reported at the r.h.s. of the figure.

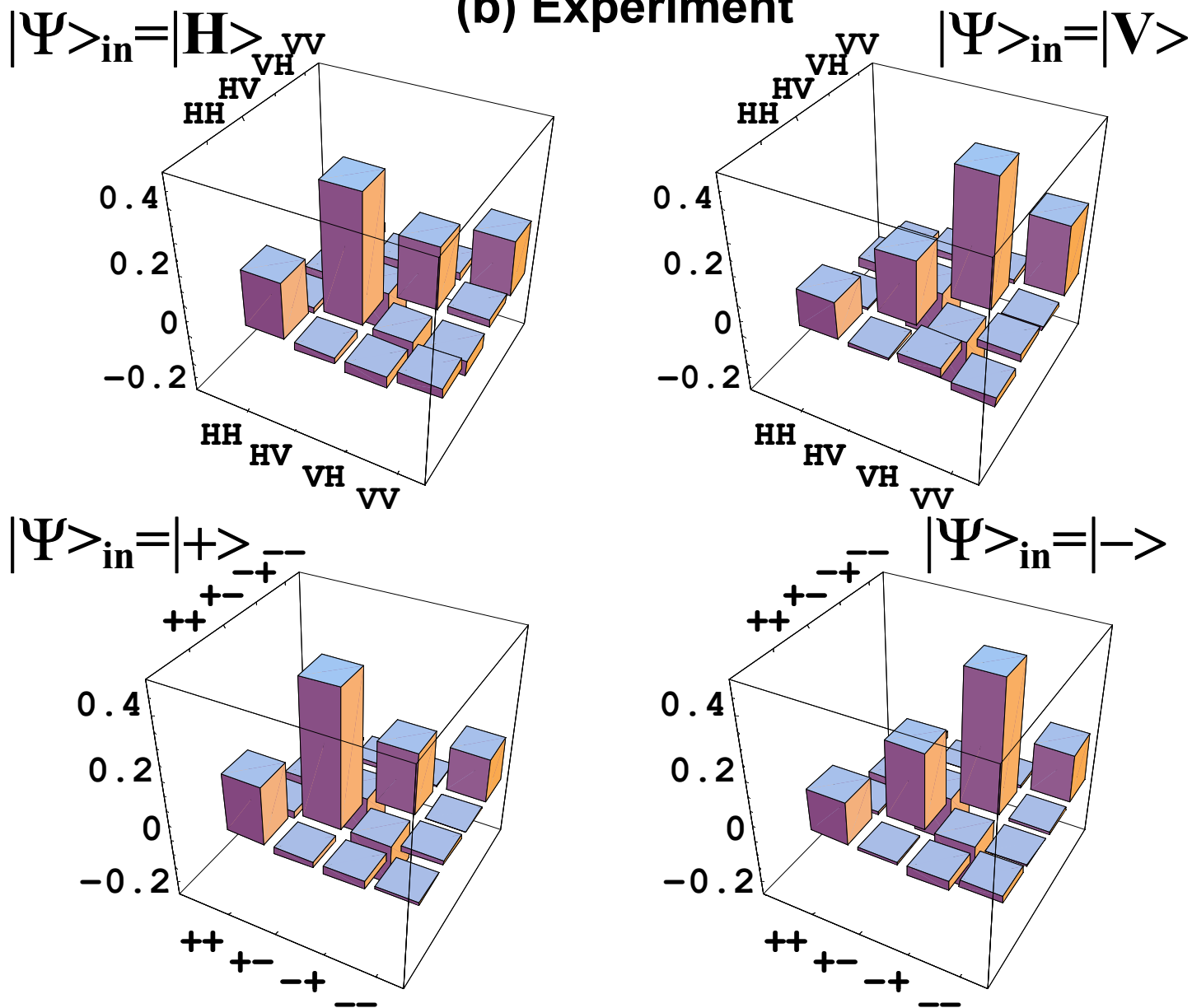


# 2-mode tomography

(a) Theory

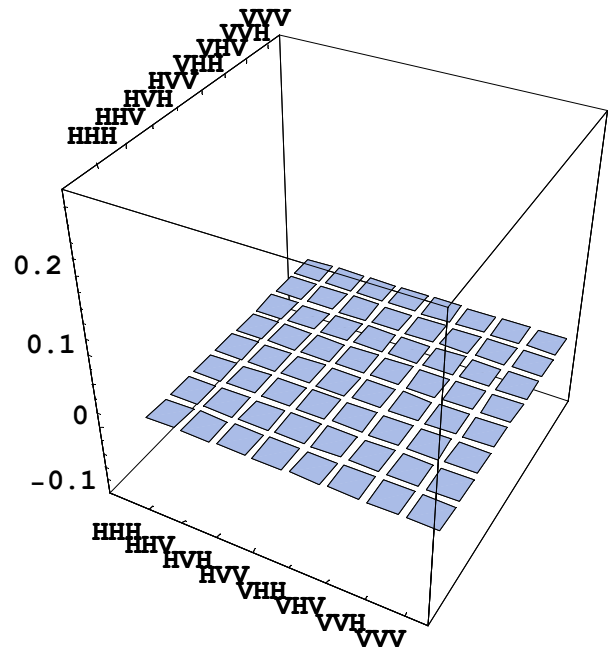
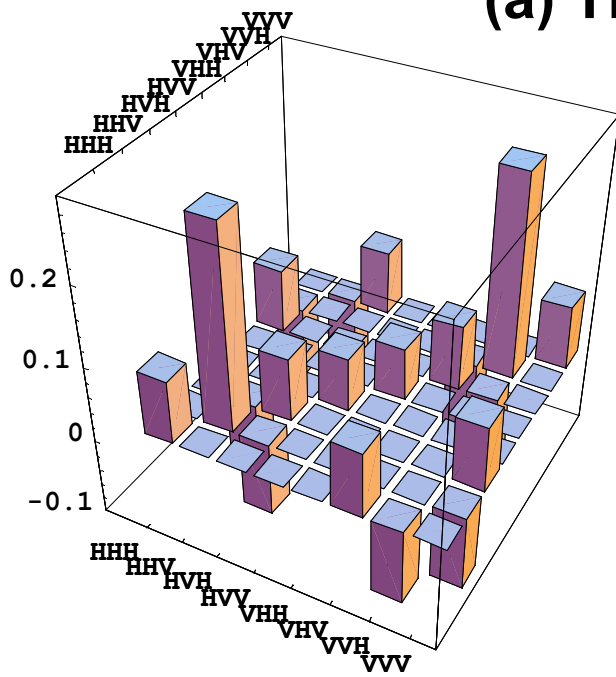


(b) Experiment



# 3-mode tomography

(a) Theory



(b) Experiment

